

## Defects Distribution of Metallocene and $\text{MgCl}_2$ -Supported Ziegler-Natta Isotactic Poly(propylenes) as Revealed by Fractionation and Crystallization Behaviors

Rufina G. Alamo

Florida Agricultural and Mechanical University and Florida State University  
College of Engineering, Department of Chemical Engineering, Tallahassee,  
FL 32310, USA

**Summary:** The inter and intramolecular distribution of defects of poly(propylenes) of the Ziegler-Natta (ZN) and metallocene (M) types, with matched molar masses and overall defect concentrations, are inferred from the crystallization and polymorphic behavior of their narrow molecular mass fractions. The fractions obtained from the M-iPP display a range in molecular masses but the same concentration of defects and provide direct evidence of the uniform intermolecular defect distribution and the “single site” nature of the catalyst. The stereodefects of the ZN-iPP fractions are more concentrated in the low molecular mass fractions, corroborating a broad interchain distribution of the nonisotactic content. In addition, the invariance of the linear growth rates among the ZN fractions and very low contents of the gamma polymorph, developed even by the most defected ZN fraction, are consistent with a stereo blocky intramolecular distribution of defects in the ZN-iPP molecules. In contrast to the linear growth rates, which are sensitive to the defect microstructure, the overall crystallization rates correlate with nucleation density and not necessarily with the iPP chain microstructure.

**Keywords:** crystallization; defect distribution; growth rates; metallocene; poly(propylene); Ziegler-Natta

### Introduction

The type and activity of reactive centers that control the mechanisms of stereo control, and hence the absolute distribution of chain defects, in the polymerization of propene with Ziegler-Natta (ZN) catalysts has been an issue of intense study.<sup>[1-4]</sup> These highly reactive species are practically inaccessible to direct observation<sup>[5]</sup> and, almost invariably, their nature has been inferred by a  $^{13}\text{C}$  NMR analysis of the polymer stereosequence distribution. The generality of the defect distribution has been hampered because, historically, ZN catalysts have been modified to increase the isotacticity level. Coupled to these modifications is a possible change in the mechanism that dictates stereospecificity and a reduced sensitivity in

the spectroscopic detection of stereosequences. Consequently, the influence of a catalyst in the defect microstructure is often reevaluated as higher field NMR spectrometers, with higher resolution and sensitivity, become available.<sup>[6-13]</sup>

The statistics of stereo control in the polymerization are often inferred by fitting the experimental  $^{13}\text{C}$  NMR stereosequences (triads, pentads, heptads, nonads) with combinations of simple limiting statistical models, each model using random statistics.<sup>[14-15]</sup> Two states models proposed independently by Chujo<sup>[16]</sup> and Doi<sup>[17]</sup>, are most frequently used to compute the components of symmetric (syndiotactic and atactic) and asymmetric (isotactic) sequences that are associated with sites that exhibit “chain-end” control or enantiomorphic site control respectively. More recently, this simple two state combination model has been found to be inappropriate to describe high resolution NMR data of ZN fractions.<sup>[18, 19]</sup> Moreover, a better agreement between the experimental and calculated stereosequence distribution was obtained in terms of three-state models that allow for reversible switches between two enantiomorphic control sites.<sup>[18-19]</sup> Such switches were associated with C1 symmetric-like active species that display 2 sites, one of them highly enantioselective.<sup>[18, 20]</sup> Fitting the experimental stereosequences to such a three state model, it was concluded that high and low tactic fractions of late generation ZN-iPPs display the same three types of stereosequences or building blocks. The difference between the fractions lies in the content of each stereosequence but not the type.

The influence of the type of catalyst and polymerization process on microstructures of industrial ZN poly(propylene)s has been classically studied by fractionation and  $^{13}\text{C}$  NMR analysis of the fractions.<sup>[21-24]</sup> TREF<sup>[22, 23]</sup> and solvent gradient extraction<sup>[11]</sup> led to fractions of increasing isotacticity and increasing molar mass, a result that clearly indicated a non uniform inter chain composition of defects, otherwise then expected from the inferred multiplicity of sites. It was also observed that most of the fractions contained syndiotactic *rrrr* pentads and, as in other works,<sup>[10-13, 21, 25]</sup> it was proposed that some of the propagation errors were “blocky” in nature. Thus, the presence of stereoblocks in the ZN-iPP has been inferred or suspected by most previous investigators and emphasized in Busico et al.’s latest work.<sup>[18]</sup>

On the basis of TREF elution profiles and degree of isotacticity of the individual fractions, Morini et al.<sup>[22]</sup> subdivided ZN-based iPPs into four major inter-molecular components: highly isotactic, mainly isotactic, stereoblocks and atactic. The fractional contents of each

component in the poly(propylenes) were found to be a strong function of the type of donor. However, the properties of the individual fractions were not studied and, as a consequence, nothing could be inferred about the defect distribution within each fraction.

The question that is most difficult to address by analysis of the NMR spectra or from the fractionation results is the nature of the intramolecular defect distribution, i.e. if the defects within a given chain deviate strongly from the random distribution. To address this issue some investigators have fitted the experimental stereosequences with models that use first order Markovian statistics for at least the symmetric chain component,<sup>[13]</sup> while in other examples the data were analyzed using a Coleman-Fox “two-state” statistical model.<sup>[10]</sup> A drawback in any of these fittings is that the experimental NMR data of the stereosequences comes from very short sequences (up to a nonad distribution). Thus stereodefects that terminate continuous isotactic sequences of 10 units or 1,000 units are indistinguishable. Any inference of a non-random intramolecular distribution of stereodefects must be obtained from the properties of the poly(propylene) fractions. We found these indirect analyses missing in the majority of earlier works dealing with elucidating distributions of stereo defects in ZN poly(propylenes). Only in one recent work was the distribution of defects in ZN-iPP considered to be blocky after comparing the content of gamma phase developed in ZN-iPP fractions and metallocene-iPPs with matched average defects compositions.<sup>[26]</sup>

The metallocene catalyst, on the other hand, leads to poly(propylenes) with uniform interchain defect composition and random intramolecular distribution.<sup>[27-29]</sup> These poly(propylenes), or their fractions, serve as models with which the properties of ZN fractions can be compared. Hence, in addition to the inferred intermolecular distribution by TREF, GPC and NMR data of ZN-iPP fractions, their adherence to or deviation from the behavior of a matched metallocene-iPP can probe the intramolecular defect distribution of the ZN-iPP molecules. In this work we use a property that is highly sensitive to defect distribution, the crystallization rates, to infer the intramolecular distribution of defects in the ZN-iPP. Moreover, the behavior of fractions from the metallocene-iPP should provide direct evidence of the uniform interchain distribution of defects and the single site nature of the catalyst.

From a crystallization perspective, the defects of the poly(propylene) chain confer a copolymeric character to the molecule. Theoretical accounts of the crystallization and melting of these “copolymers” have been undertaken from phase equilibrium consideration involving

more than one species.<sup>[30]</sup> When defects are rejected from the crystal, the equilibrium melting/crystallization temperature does not depend directly on the composition of the copolymer but rather upon the sequence distribution of crystallizable sequences. The sequence distribution probability ( $p$ ) of a block copolymer is one. This requires that there is no depression in the melting or crystallization of block copolymers with increasing lengths or numbers of blocks. The unchanged undercooling leads to constant crystallization rates. Conversely, the parameter  $p$  of a random copolymer is less than one and, on equilibrium considerations, melting or crystallization are largely depressed with increasing concentration of defects in the chain. The change in undercooling affects the crystallization kinetics of these copolymers accordingly. These theoretical accounts give the basis for the above mentioned comparisons. Experimental work was aimed at distinguishing intramolecular stereoblock-like versus a random-like distribution of defects in the ZN fractions from analysis of their crystallization rates compared with those from matched fractions of a metallocene-iPP. In addition and as separate work,  $^{13}\text{C}$  NMR stereosequences of fractions were theoretically analyzed using two state and three state statistical models for conformity with the observed crystallization rates.<sup>[19]</sup>

## Experimental

A ZN-iPP obtained with a fourth generation  $\text{MgCl}_2$  – supported industrial catalyst using an alkylphthalate-type internal donor and alkoxysilane-type external donor, and a metallocene catalyzed iPP were fractionated via supercritical fluid extraction in *n*-propane by increasing pressure, at a constant temperature of  $150^\circ\text{C}$ .<sup>[31, 32]</sup> Both poly(propylenes) have matched mass average molecular mass and the same 0.51 mol% overall concentration of all type of defects, the latter measured from the  $^{13}\text{C}$  NMR spectra. The content of stereo defects was taken as half the fraction of *mmmr* pentads and the *erythro* 2,1 regio defects calculated from the  $^{13}\text{C}$  NMR resonances characteristic of this group. Characterization data of the unfractionated parents and their fractions are listed in Table 1.

The linear growth rates ( $G$ ) were followed in an Olympus BH2 polarized optical microscope fitted with a Linkam hot stage, TP-93. The calculated uncertainty in the value of  $G$  was very low ( $\pm 0.01 \times 10^{-6}$  cm/s). Overall crystallization rates were taken as the inverse of the time required for 50% of the transformation to take place. The degree of transformation, at fixed

isothermal temperature, was followed by the variation of the heat flow vs. time in a Perkin Elmer DSC-7. WAXD patterns were recorded at room temperature in a Phillips X' Pert PW 3040 MRD diffractometer.

Table 1. Characterization of parent polymers and fractions from Metallocene and ZN-iPP.

Sample	Mw (g/mol)	Mw/Mn	stereo defects (mol%)	regio defects (mol%)	Total defects (mol%)	Tm (°C) <sup>(a)</sup>	ΔH (J/g) <sup>(a)</sup>
M203K0.51 parent	203,900	2.00	0.11	0.40	0.51	155.0	76.0
Mf86K0.56	86,000	1.43	0.16	0.40	0.56	156.2	85.7
Mf121K0.50	121,000	1.32	0.11	0.39	0.50	156.3	75.2
Mf143K0.54	143,000	1.24	0.07	0.47	0.54	156.1	86.0
Mf200K0.46	200,000	1.23	0.08	0.38	0.46	155.8	80.4
Mf235K0.45	235,000	1.24	0.07	0.38	0.45	154.6	93.1
Mf358K0.41	358,000	1.34	0.07	0.34	0.41	154.0	73.5
Mf383K0.41	383,000	1.47	na <sup>(b)</sup>	na	na	na	
Z263K0.51 parent	262,600	3.19	0.51	---	0.51	161.4	79.4
Zf97K1.03	97,000	1.31	1.03	---	1.03	159.0	89.6
Zf163Kxxx	157,000	1.27	Na	---	na	na	
Zf163K0.60	163,000	1.97	0.60	---	0.60	161.3	80.5
Zf204K0.41	204,000	2.15	0.41	---	0.41	160.9	81.6
Zf328K0.36	328,000	1.77	0.36	---	0.36	162.3	81.5

(a) Rapidly quenched samples to 25 °C. Tm: Peak melting temperature, ΔH: Heat of fusion

(b) Data not available.

## Results and Discussion

Both fractionations of the parents iPPs display a systematic increase of the molar mass of the fractions with increasing pressure, as seen in Table 1, indicating that the fractionation took place preferentially by molecular mass. The concentration of defects of the metallocene fractions is basically constant within the series, providing direct evidence of the narrow inter-chain composition distribution of the M-iPP. However, as the molar mass of the ZN-iPP fractions increase, the defect concentration decreases from 1.03 to 0.36 mol% respectively, evidencing the expected inter-chain heterogeneity of defect distribution in the parent ZN-iPP. Similar trends have been observed in ZN-iPP using other fractionation procedures.<sup>[21-24]</sup> The ZN-iPP contains a fraction of highly isotactic long molecules which are not present in the metallocene-iPP. The results from each fractionation explain the observed differences in

isothermal linear growth rates of the unfractionated matched po(lypropylenes) (Figure 1A). At any crystallization temperature, the spherulites of the unfractionated ZN-iPP grow at about twice the rate of the metallocene-iPP. The ZN-iPP crystallites melt at  $\sim 8^\circ\text{C}$  higher than metallocene-iPP crystals (Figure 1B). Thus, it appears that the longer isotactic sequences found in the ZN-iPP are selected earlier during crystallization and lead to a fraction of thicker crystallites that melt at higher temperatures than the crystals formed from the more uniformly distributed M-iPP. Moreover, it was found that the nucleation density of M-iPP is significantly higher than that of ZN-iPP, perhaps due to residues in the melt from the metallocene catalyst. Since overall crystallization rates are a direct function of the primary nucleation density, the overall crystallization rates of M-iPP were found faster than those of the ZN-iPP. As a consequence of nucleation differences, on cooling from the melt at a constant rate of  $10^\circ\text{C}/\text{min}$ , the heat of crystallization evolves faster for M-iPP as seen in Figure 1C. Any measured overall crystallization rate would correlate with nucleation density and not necessarily with the microstructure of the iPP molecules.

The fractionation results alone do not allow conclusions about the nature of the intramolecular defect distribution. This issue can only be inferred after analysis of the properties of the individual fractions.

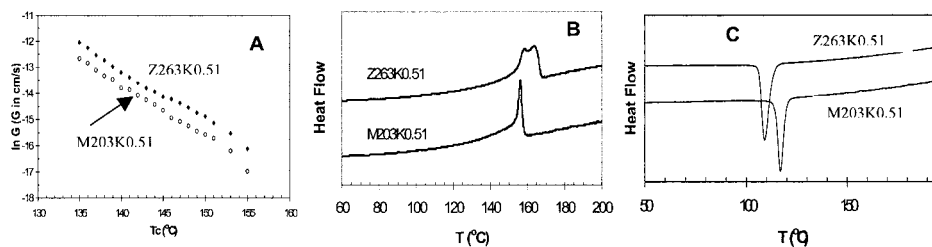


Figure 1. Properties of unfractionated iPPs. A. Isothermal linear growth rates, B. DSC melting C. DSC crystallization at  $10^\circ\text{C}/\text{min}$ .

## Crystallization of Metallocene iPPs

Figure 2 shows the spherulitic linear growth rates of the metallocene fractions, measured isothermally in a temperature range between  $134^\circ\text{C}$  and  $155^\circ\text{C}$ . The rates follow the strong negative temperature coefficient dictated by nucleation and growth theories.<sup>[33, 34]</sup> The

observed small but systematic decrease of the rate with molecular mass, at a fixed crystallization temperature, follows the pattern of other homopolymers and copolymers.<sup>[34-36]</sup> The change in the rate is pronounced only when crystallization can be followed at low undercoolings,<sup>[33,34]</sup> large variations with molar mass are not expected at the relatively high undercoolings ( $>30^{\circ}\text{C}$ ) at which crystallization of iPP is observed. The variation of the rate with molar mass is attributed to the increased number of entanglements per chain in the melt, which affect segmental transport in the crystallization process.

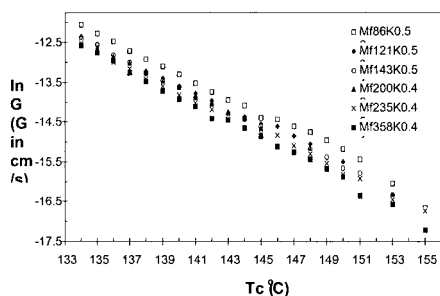


Figure 2. Linear growth rates of molecular mass fractions of M-iPP as function of  $T_c$ .

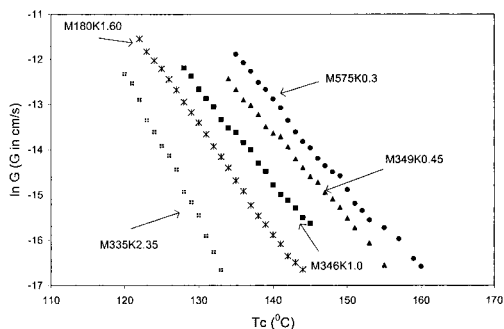


Figure 3. Linear growth rates of M-iPPs with different concentration of defects.

Homogeneous metallocene poly(propylenes), with stereo ( $\sim\text{mrrm}\sim$ ) and regio (2, 1 type) defects were studied to guide the variation of growth rates with concentration of defects.<sup>[37]</sup> The linear growth rates for a series of M-iPPs with total defect content increasing from 0.30 to 2.35 mol% are given in Figure 3. The growth rate decreases about two orders of magnitude when the total defect content is increased in the range studied. This strong effect on the rate reflects the overall inhibition of the crystallization process imposed by the stereo ( $\sim\text{mmrrm}\sim$ ) and 2,1 regio defects despite their partial inclusion in the lattice.<sup>[38]</sup> An increase in non-crystallizable structural irregularities leads to a reduction of the amount of crystallizable sequences and, thus, to a decrease in the crystallization rate.<sup>[35, 37]</sup> This behavior is analogous to the overall crystallization rates of a series of random ethylene copolymers.<sup>[35]</sup> For these copolymers the rate was also found to decrease about 2 orders of magnitude with increasing concentration of branch points from 1.21 to 2.3 mol %.

## Crystallization of ZN-iPP fractions

Isothermal linear growth rates of the ZN-iPP fractions are given in Figure 4. Compared to those of the metallocene fractions there is no systematic variation of  $G$  with either molar mass or concentration of defects, despite a variation in defects from 0.36 to 1.03 mol% among the ZN fractions. Should the defects in each ZN fraction be randomly distributed, one would have expected a significantly lower  $G$  for the fraction with 1.03 mol% defects, as indicated by the behavior of metallocene-iPPs in Figure 3. Furthermore, there are only minor differences between the growth rates of any ZN-iPP fraction at a fixed crystallization temperature. This experimental fact can only be reconciled with a defect distribution that deviates from the random defect distribution of the metallocene fractions and that is propagated among all the ZN-iPP fractions. The invariance of the linear growth rates among the ZN fractions is consistent with a stereo blocky intramolecular distribution of defects in all ZN-iPP molecules. One could argue that the expected decrease of  $G$  with increasing defect content in the ZN fractions may be compensated by an opposite effect of molar mass on  $G$ . However, appropriate corrections to the data of figure 4 for constant molecular mass did not cause any significant variation in the data or trends of the rates shown in figure 4.<sup>[39]</sup>

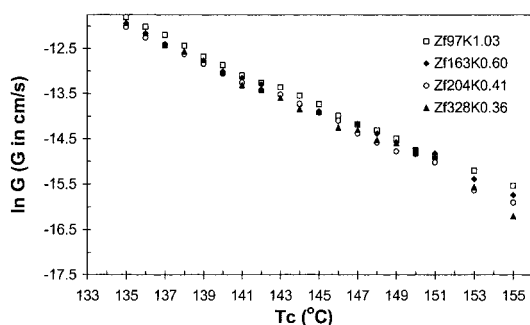


Figure 4. Linear growth rates of molecular mass fractions of ZN-iPP as function of  $T_c$ .

Additional evidence, which supports the stereoblock nature of the ZN-iPP chains, is found in the significantly low contents of gamma polymorph that ZN-iPP fractions develop compared to metallocene-iPPs with matched concentrations of defects. A metallocene-iPP with a concentration of 1.0 mol% of defects homogeneously distributed, crystallized at 125°C,



develops about 50% crystallites in the  $\gamma$  polymorph and the other half in the  $\alpha$  form.<sup>[39, 40]</sup> The more defected ZN fractions (Z97K1.03 and Zf163K0.6) develop only about 10% of the  $\gamma$  polymorph at the same crystallization temperature. These results prove that the required presence of short crystallizable sequences for the formation of the  $\gamma$  polymorph is fulfilled in the metallocene-iPP with a random distribution of defects but not in the ZN fractions. Significantly lower contents of the gamma phase are expected in molecules where long isotactic sequences join blocks of poorly stereo regular sequences, as schematically shown in Figure 5. In this microstructural model for ZN-iPP, the intermolecular defect composition is non-uniform with the shorter chains having a higher concentration of non isotactic units so as to comply with the fractionation behavior. However, the intramolecular distribution of defects is blocky. All chains display similar types of long crystallizable sequences, which are highlighted in the schematic figure. Accordingly, molecular fractions from this model are expected to show negligible differences in crystallization rates. The experimental growth rates and polymorphic behavior of ZN-iPP fractions conform with this structural model. Stereoblock distributions in various types of iPPs have been also inferred in other works by analysis of their polymorphic behavior.<sup>[26, 41]</sup>

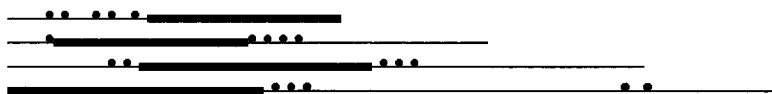


Figure 5. Model for stereosequence distribution in parent ZN-iPP.

## Conclusions

Classical fractionation and  $^{13}\text{C}$  NMR characterization of individual fractions of matched ZN-iPP and M-iPP have been carried out to determine the intermolecular distribution of defects in the iPP chains. These methods have been combined with analysis of the linear growth rates of the fractions, a useful tool to infer the intramolecular defect distribution in the ZN-iPP chains. The fractions from the M-iPP display a range in molecular mass but the same defect concentration. These fractions provide evidence of the uniform inter-chain defect distribution in this poly(propylene). The linear growth rates of the M-iPP fractions only reflect differences

due to the molecular mass effect on the crystallization rate and, thus, are consistent with a random intramolecular distribution of defects.

The molar fractions obtained from the ZN-iPP confirmed that the content of defects is broadly distributed on an intermolecular basis. In addition, the basically identical growth rates found in all ZN fractions and the formation of very low contents of the gamma polymorph, even in the most defected fraction, is consistent with a stereoblocky intramolecular distribution of defects. A schematic model of this distribution has been proposed.

## Acknowledgements

This work was supported by the National Science Foundation (DMR-0094485). Contributions to this work by J.C. Randall, J.A. Blanco, S. Putcha, C. Chi, P.K. Agarwal, C.J. Ruff, E. Ritchson and D. Li are acknowledged.

- [1] E. Albizzati, U. Giannini, G. Collina, L. Noristi, L. Resconi in *Polypropylene Handbook. Part I. Catalysts and Polymerizations* E.P. Moore Jr., Hanser Pub. **1996**.
- [2] V. Busico, R. Cipullo, *Prog. Polym. Sci.* **2001**, *26*, 443.
- [3] J.C. Chadwick, G. Morini, G. Balbontin, I. Camurati, J.J.R. Heere, I. Mingozzi, F. Testoni, *Macromol. Chem. Phys.* **2001**, *202*, 1995.
- [4] M.C. Sacchi, F. Forlini, I. Tritto, P. Locatelli, G. Morini, L. Noristi, E. Albizzati, *Macromolecules* **1996**, *29*, 3341.
- [5] V. Busico, R. Cipullo, F. Cutillo, M. Vacatello, *Macromolecules* **2002**, *35*, 349.
- [6] A. Zambelli, P. Locatelli, G. Bajo, F.A. Bovey, *Macromolecules* **1975**, *8*, 687.
- [7] A. Zambelli, P. Locatelli, A. Provasoli, D.R. Ferro, *Macromolecules* **1980**, *13*, 267.
- [8] H. Kawamura, T. Hayashi, Y. Inoue, R. Chujo, *Macromolecules* **1989**, *22*, 2181.
- [9] V. Busico, P. Corradini, L. De Martino, F. Graziano, A.M. Iadicicco, *Makromol. Chem.* **1991**, *192*, 49.
- [10] V. Busico, P. Corradini, R. De Biasio, L. Landriani, A.L. Segre, *Macromolecules* **1994**, *27*, 4521.
- [11] V. Busico, R. Cipullo, P. Corradini, L. Landriani, M. Vacatello, *Macromolecules* **1995**, *28*, 1887.
- [12] V. Busico, R. Cipullo, G. Talarico, A.L. Segre, J.C. Chadwick, *Macromolecules* **1997**, *30*, 4786.
- [13] J.C. Randall, *Macromolecules* **1997**, *30*, 803.
- [14] R.A. Shelden, T. Fueno, T. Tsunetsugu, J. Furukawa, *J. Polym. Sci., Part A*, **1965**, *3*, 23.
- [15] F.A. Bovey, G.V.D. Tiers, *J. Polym. Sci.* **1960**, *44*, 173.
- [16] R. Chûjô, *Kagaku* **1981**, *36*, 420.
- [17] Y. Doi, *Makromol. Chem., Rapid Commun.* **1982**, *3*, 635.
- [18] V. Busico, R. Cipullo, G. Monaco, G. Talarico, M. Vacatello, J.C. Chadwick, A.L. Segre, O. Sudmeijer, *Macromolecules* **1999**, *32*, 4173.
- [19] J.C. Randall, R.G. Alamo, P.K. Agarwal, C.J. Ruff, *Macromolecules* **2003**, *36*, 1572.
- [20] V. Busico, R. Cipullo, C. Polzone, G. Talarico, J.C. Chadwick, *Macromolecules* **2003**, *36*, 2616.
- [21] R. Paukkeri, T. Vaananen, A. Lehtinen, *Polymer* **1993**, *34*, 2488.
- [22] G. Morini, E. Albizzati, G. Balbontin, I. Mingizzi, M.C. Sacchi, F. Forlini, I. Tritto, *Macromolecules* **1996**, *29*, 5770.
- [23] P. Viville, D. Daoust, A.M. Jonas, B. Nysten, R. Legras, M. Dupire, J. Michel, G. Debras, *Polymer*, **2001**, *42*, 1953.
- [24] J. Xu, L. Feng, S. Yang, X. Kong, *Eur. Polym. J.* **1998**, *34*, 431.
- [25] J.C. Chadwick, A. Miedema, B.J. Ruisch, O. Sudmeijer, *Makromol. Chem.* **1992**, *193*, 1463.
- [26] F.P.T.J. van der Burgt, S. Rastogi, J.C. Chadwick, B. Rieger, *J. Macromol. Sci. Phys.* **2002**, *B41*, 1091.

- [27] M. Farina, G. Di Silvestro, A. Terragni, *Macromol. Chem. Phys.* **1995**, 196, 353.
- [28] H.H. Brintzinger, D. Fischer, R. Mulhaupt, B. Rieger, R.M. Waymouth, *Angew Chem. Int. Ed. Engl.* **1995**, 34, 1143.
- [29] L. Resconi, L. Cavallo, A. Fait, F. Piemontesi, *Chem. Rev.* **2000**, 100, 1253.
- [30] P.J. Flory, *Trans. Faraday Soc.* **1955**, 51, 848.
- [31] J.J. Watkins, V.J. Krukonis, P.D. Condo, Jr., D. Pradhan, P. Ehrlich, *J. Supercritical Fluids* **1991**, 4, 24.
- [32] L.J.D. Britto, J.B. P. Soares, A. Peulidis, V. Krukonis, *J. Polym. Sci., Polym. Phys. Ed.* **1999**, 37, 553.
- [33] J.D. Hoffman, L.J. Frolen, G.S. Ross, J.I. Lauritzen, *J. Res. Natl. Bur. Stand.* **1975**, 79A, 671.
- [34] E. Ergoz, J.G. Fatou, L. Mandelkern, *Macromolecules* **1972**, 5, 147.
- [35] R.G. Alamo, L. Mandelkern, *Macromolecules* **1991**, 24, 6480.
- [36] L.C. Lopez, G.L. Wilkes, *Polymer* **1988**, 29, 106.
- [37] R.G. Alamo, C. Chi, Crystallization Behavior and Properties of Polyolefins. In *Molecular Interactions and Time-Space Organization in Macromolecular Systems*; Y. Morishima, T. Norisuye, K. Tashiro, Eds.; Springer: Berlin **1999**; p. 29.
- [38] D.L. VanderHart, R.G. Alamo, MR. Nyden, M.H. Kim, L. Mandelkern, *Macromolecules* **2000**, 22, 6078.
- [39] R.G. Alamo, J.A. Blanco, P.K. Agarwal, J.C. Randall, *Macromolecules* **2003**, 36, 1559.
- [40] R.G. Alamo, M.H. Kim, M.J. Galante, J.R. Isasi, L. Mandelkern, *Macromolecules* **1999**, 32, 4050.
- [41] C. De Rosa, F. Auriemma, T. Circelli, R.M. Waymouth, *Macromolecules* **2002**, 35, 3622.

